Influence of Traction Transmission System on Hunting Stability of Train Bogie System

Yuewei Yu, Leilei Zhao, Yirui Zhang, Chuanbo Ma and Boao Yan

***Abstract*—For the purpose of investigating the dynamic coupling mechanism between the high-speed train's bogie hunting stability and the traction motor and gearbox, a power bogie hunting motion model that comprehensively considers the coupling interaction between the traction motor, gearbox, and bogie frame is proposed. The model is verified through vehicle simulation. Based on this, according to Routh-Hurwitz stability criterion, the influences of traction motor and gearbox's vibration isolation parameters as well as the coupling's performance parameters on power bogie's hunting stability are discussed. This research provides a model reference for power bogie's hunting motion stability analysis, and also provides a theoretical guidance for the design of traction motor and gearbox's suspension parameters.**

***Index Terms*—power bogie, traction motor, gearbox, hunting motion, stability analysis**

I. INTRODUCTION

The stability of bogie's hunting motion is crucial for train's safe operation [1,2]. Recently, a large number of scholars have carried out plentiful valuable research work in this aspect. However, the hunting motion models established in these studies are all aimed at trailer bogies [3-6], and are difficult to effectively characterize power bogie (PB) system's hunting motion characteristics containing traction transmission components. In order to solve this problem, many scholars have done valuable work on PB system's hunting stability [7-13]. However, these studies only considered the impact of traction motors on the bogie frame. In fact, for high-speed train's PB, its traction transmission components not only contains the traction motor, but also the gearbox, both of them have a great effect on bogie frame's dynamic performance [14,15]. Only by integrating the traction motor, gearbox, as well as bogie frame into a whole system for research can the stability characteristics of the PB system be effectively characterized, but there is still a lack of systematic and in-depth research in this aspect.

In this paper, based on the comprehensive consideration of the coupling interaction between the traction motor, gearbox, and bogie frame, a high-speed train's PB hunting motion model containing traction transmission components is established, meanwhile, the influences of traction motor and gearbox's vibration isolation parameters as well as the coupling's performance parameters on PB system's hunting stability are discussed.

II. HUNTING MOTION MODEL OF THE PB SYSTEM

A. Physical model

The stability of bogie's hunting motion belongs to lateral dynamics problem and has little to do with its vertical degrees of freedom. Thus, when establishing the hunting motion model of a bogie system, only its lateral and yaw degrees of freedom are usually considered [16]. In addition, during the bogie's hunting motion, the car body is almost stationary. Therefore, for the purpose of facilitating mathematical modeling, when studying bogie system's hunting stability, the vibration of the car body is usually not considered, and only the lateral movement of the bogie system is taken into account [12]. In view of this, in order to effectively characterize the PB system's hunting stability characteristics, a hunting motion model for PB systems that comprehensively considers the coupling interaction between the traction motor, gearbox, and bogie frame is proposed, as shown in Figure 1. Here, the model includes the lateral and yaw movements of the bogie frame, traction motor, wheel-set, and gearbox, as well as the end elastic deformation of the yaw damper, traction motor lateral damper, and secondary lateral damper [17], totaling 30 degrees of freedom, specifically: the bogie frame's lateral and yaw displacements y_b and φ_b; the first traction motor's lateral and yaw displacements y_{m1} and φ_{m1}; the second traction motor's lateral and yaw displacements y_{m2} and φ_{m2}; the first gearbox's lateral and yaw displacements y_{g1} and φ_{g1}; the second gearbox's lateral and yaw displacements y_{g2} and φ_{g2}; the first wheel-set's lateral and yaw displacements y_{w1} and φ_{w1}; the second wheel-set's lateral and yaw displacements y_{w2} and φ_{w2}; the traction motor lateral damper's piston rod displacements y_{e1}~y_{e8}; the yaw damper's piston rod displacements x_{s1}~x_{s4}, the secondary lateral damper's piston rod displacements y_{d1}~y_{d4}. Compared with traditional PB models, this model fully considers the coupling interaction between the traction motor, gearbox, and bogie frame, which is more in line with the actual situation of the PB systems.

Manuscript received March 9, 2025; revised May 15, 2025. This work was supported in part by the National Natural Science Foundation of China (Grant No. 52305266) and the China Postdoctoral Science Foundation Project (Grant No. 2023M732628).

Yuewei Yu is an associate professor of the School of Transportation and Vehicle Engineering, Shandong University of Technology, Zibo 255000, China (corresponding author, e-mail: yuyuewei2010@163.com).

Leilei Zhao is an associate professor of the School of Transportation and Vehicle Engineering, Shandong University of Technology, Zibo 255000, China (e-mail: zhaoleilei611571@163.com).

Yirui Zhang is a lecturer of the School of Transportation and Vehicle Engineering, Shandong University of Technology, Zibo 255000, China (e-mail: zyr86913@163.com).

Chuanbo Ma is a postgraduate of the School of Transportation and Vehicle Engineering, Shandong University of Technology, Zibo 255000, China (e-mail: 1340909445@qq.com).

Boao Yan is a postgraduate of the School of Transportation and Vehicle Engineering, Shandong University of Technology, Zibo 255000, China (e-mail: 1549797465@qq.com).

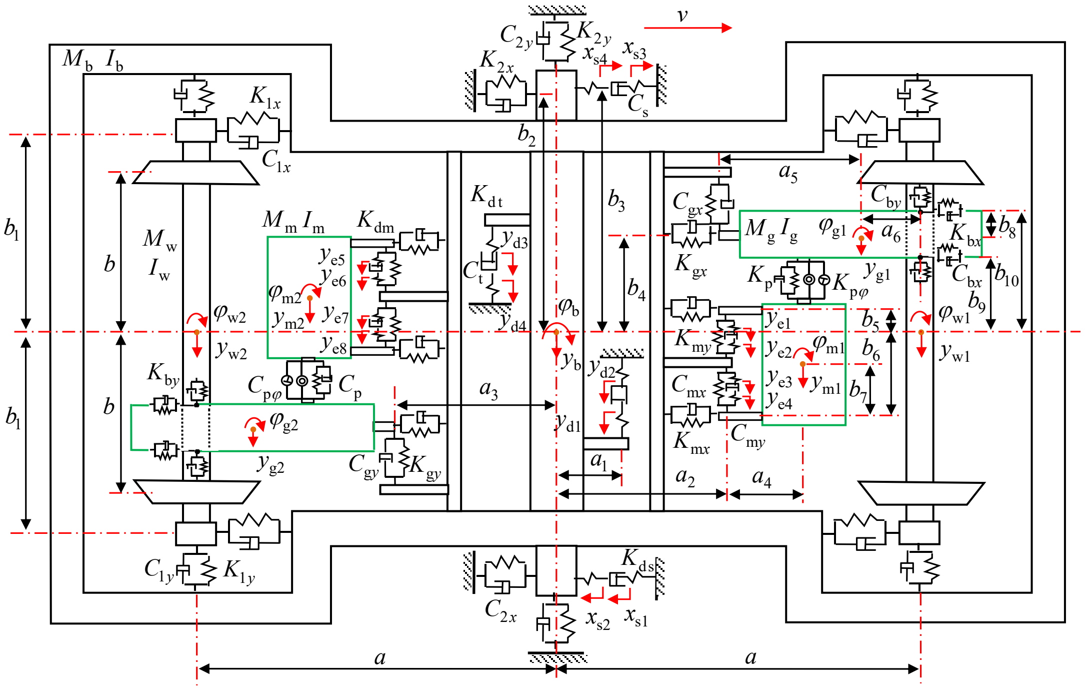

Fig. 1. Hunting motion model of PB systems considering the influence of traction transmission components

In Figure 1, M_b, M_w, M_m, and M_g represent the mass of each bogie frame, wheel-set, traction motor, and gearbox; I_b, I_w, I_m and I_g represent the yaw moment of inertia of each bogie frame, wheel-set, traction motor, and gearbox; K_{1x}, K_{1y} and C_{1x}, C_{1y} are each axle box suspension system's longitudinal and lateral stiffness and damping; K_{2x}, K_{2y} and C_{2x}, C_{2y} are the secondary suspension's longitudinal and lateral stiffness and damping; C_s, C_t, and C_{my} represent the damping of the yaw damper, secondary lateral damper, and traction motor lateral damper; K_{ds}, K_{dt}, and K_{dm} are the end connection stiffness of the yaw damper, secondary lateral damper, and traction motor lateral damper; K_{gx}, K_{gy} and C_{gx}, C_{gy} are each gearbox suspension's longitudinal and lateral stiffness and damping; K_{mx}, K_{my}, and C_{mx} are the traction motor suspension's longitudinal stiffness, lateral stiffness, and longitudinal damping; K_{bx}, K_{by} and C_{bx}, C_{by} are the longitudinal and lateral stiffness and damping of the gearbox's support bearings; K_p, $K_{p\varphi}$ and C_p, $C_{p\varphi}$ are the lateral and yaw equivalent stiffness and damping of the coupling; b is the lateral distance from the wheel-rail contact point to bogie frame's mass center; b_1, b_2, b_3, and b_4 are the lateral distances from the bogie frame mass center to the primary suspension, secondary suspension, yaw damper, and gearbox suspension; b_5 and b_6 are the lateral distances from the bogie frame mass center to the traction motor suspension system; b_7 is the lateral distance from the traction motor mass center to its suspension center; b_8 is the lateral distance from the gearbox mass center to its support bearing; b_9 and b_{10} are the lateral distances from the bogie frame mass center to the gearbox's support bearing; a is half of the wheelbase; a_1, a_2, and a_3 are the longitudinal distances between the bogie frame mass center and the secondary lateral damper, traction motor suspension, and gearbox suspension; a_4 is the longitudinal distance from the traction motor mass center to its suspension center; a_5 and a_6 are the longitudinal distances from the gearbox mass center to its suspension center and supporting bearing; v is the train speed.

B. Mathematical model

(1) The first traction motor:

$$\begin{cases} M_m\ddot{y}_{m1} - 2K_{my}(y_b + a_2\varphi_b - y_{m1} + a_4\varphi_{m1}) + \\ \quad K_{dm}(y_{m1} - a_4\varphi_{m1} - y_{e1}) + K_{dm}(y_{m1} - a_4\varphi_{m1} - y_{e4}) + \\ \quad K_p(y_{m1} - y_{g1}) + C_p(\dot{y}_{m1} - \dot{y}_{g1}) = 0 \\ I_m\ddot{\varphi}_{m1} + 2K_{my}a_4(y_b + a_2\varphi_b - y_{m1} + a_4\varphi_{m1}) - \\ \quad K_{dm}a_4(y_{m1} - a_4\varphi_{m1} - y_{e1}) - K_{dm}a_4(y_{m1} - a_4\varphi_{m1} - y_{e4}) + \\ \quad K_{mx}b_7(b_7\varphi_{m1} - b_5\varphi_b) + C_{mx}b_7(b_7\dot{\varphi}_{m1} - b_5\dot{\varphi}_b) + \\ \quad K_{mx}b_7(b_7\varphi_{m1} - b_6\varphi_b) + C_{mx}b_7(b_7\dot{\varphi}_{m1} - b_6\dot{\varphi}_b) + \\ \quad K_{p\varphi}(\varphi_{m1} - \varphi_{g1}) + C_{p\varphi}(\dot{\varphi}_{m1} - \dot{\varphi}_{g1}) = 0 \end{cases} \tag{1}$$

(2) The second traction motor:

$$\begin{cases} M_m\ddot{y}_{m2} - 2K_{my}(y_b - a_2\varphi_b - y_{m2} - a_4\varphi_{m2}) + \\ \quad K_{dm}(y_{m2} + a_4\varphi_{m2} - y_{e5}) + K_{dm}(y_{m2} + a_4\varphi_{m2} - y_{e8}) + \\ \quad K_p(y_{m2} - y_{g2}) + C_p(\dot{y}_{m2} - \dot{y}_{g2}) = 0 \\ I_m\ddot{\varphi}_{m2} - 2K_{my}a_4(y_b - a_2\varphi_b - y_{m2} - a_4\varphi_{m2}) + \\ \quad K_{dm}a_4(y_{m2} + a_4\varphi_{m2} - y_{e5}) + K_{dm}a_4(y_{m2} + a_4\varphi_{m2} - y_{e8}) + \\ \quad K_{mx}b_7(b_7\varphi_{m2} - b_5\varphi_b) + C_{mx}b_7(b_7\dot{\varphi}_{m2} - b_5\dot{\varphi}_b) + \\ \quad K_{mx}b_7(b_7\varphi_{m2} - b_6\varphi_b) + C_{mx}b_7(b_7\dot{\varphi}_{m2} - b_6\dot{\varphi}_b) + \\ \quad K_{p\varphi}(\varphi_{m2} - \varphi_{g2}) + C_{p\varphi}(\dot{\varphi}_{m2} - \dot{\varphi}_{g2}) = 0 \end{cases} \tag{2}$$

(3) The first gearbox:

$$\begin{cases} M_g\ddot{y}_{g1} - K_{gy}(y_b + a_3\varphi_b - y_{g1} + a_5\varphi_{g1}) + K_p(y_{g1} - y_{m1}) - \\ \quad C_{gy}(\dot{y}_b + a_3\dot{\varphi}_b - \dot{y}_{g1} + a_5\dot{\varphi}_{g1}) + C_p(\dot{y}_{g1} - \dot{y}_{m1}) + \\ \quad 2K_{by}(y_{g1} + a_6\varphi_{g1} - y_{w1}) + 2C_{by}(\dot{y}_{g1} + a_6\dot{\varphi}_{g1} - \dot{y}_{w1}) = 0 \\ I_g\ddot{\varphi}_{g1} + K_{gy}a_5(y_b + a_3\varphi_b - y_{g1} + a_5\varphi_{g1}) + K_{p\varphi}(\varphi_{g1} - \varphi_{m1}) + \\ \quad C_{gy}a_5(\dot{y}_b + a_3\dot{\varphi}_b - \dot{y}_{g1} + a_5\dot{\varphi}_{g1}) + C_{p\varphi}(\dot{\varphi}_{g1} - \dot{\varphi}_{m1}) + \\ \quad 2K_{by}a_6(y_{g1} + a_6\varphi_{g1} - y_{w1}) + 2C_{by}a_6(\dot{y}_{g1} + a_6\dot{\varphi}_{g1} - \dot{y}_{w1}) + \\ \quad K_{bx}b_8(b_8\varphi_{g1} + b_9\varphi_{w1}) + C_{bx}b_8(b_8\dot{\varphi}_{g1} + b_9\dot{\varphi}_{w1}) + \\ \quad K_{bx}b_8(b_8\varphi_{g1} - b_{10}\varphi_{w1}) + C_{bx}b_8(b_8\dot{\varphi}_{g1} - b_{10}\dot{\varphi}_{w1}) = 0 \end{cases} \tag{3}$$

(4) The second gearbox:

$$\left\{\begin{aligned}
&M_{\mathrm{g}}\ddot{y}_{\mathrm{g2}}-K_{\mathrm{g}y}(y_{\mathrm{b}}-a_3\varphi_{\mathrm{b}}-y_{\mathrm{g2}}-a_5\varphi_{\mathrm{g2}})+K_{\mathrm{p}}(y_{\mathrm{g2}}-y_{\mathrm{m2}})-\\
&\quad C_{\mathrm{g}y}(\dot{y}_{\mathrm{b}}-a_3\dot{\varphi}_{\mathrm{b}}-\dot{y}_{\mathrm{g2}}-a_5\dot{\varphi}_{\mathrm{g2}})+C_{\mathrm{p}}(\dot{y}_{\mathrm{g2}}-\dot{y}_{\mathrm{m2}})+\\
&\quad 2K_{\mathrm{b}y}(y_{\mathrm{g2}}-a_6\varphi_{\mathrm{g2}}-y_{\mathrm{w2}})+2C_{\mathrm{b}y}(\dot{y}_{\mathrm{g2}}-a_6\dot{\varphi}_{\mathrm{g2}}-\dot{y}_{\mathrm{w2}})=0\\
&I_{\mathrm{g}}\ddot{\varphi}_{\mathrm{g2}}-K_{\mathrm{g}y}a_5(y_{\mathrm{b}}-a_3\varphi_{\mathrm{b}}-y_{\mathrm{g2}}-a_5\varphi_{\mathrm{g2}})+K_{\mathrm{p}\varphi}(\varphi_{\mathrm{g2}}-\varphi_{\mathrm{m2}})-\\
&\quad C_{\mathrm{g}y}a_5(\dot{y}_{\mathrm{b}}-a_3\dot{\varphi}_{\mathrm{b}}-\dot{y}_{\mathrm{g2}}-a_5\dot{\varphi}_{\mathrm{g2}})+C_{\mathrm{p}\varphi}(\dot{\varphi}_{\mathrm{g2}}-\dot{\varphi}_{\mathrm{m2}})-\\
&\quad 2K_{\mathrm{b}y}a_6(y_{\mathrm{g2}}-a_6\varphi_{\mathrm{g2}}-y_{\mathrm{w2}})-2C_{\mathrm{b}y}a_6(\dot{y}_{\mathrm{g2}}-a_6\dot{\varphi}_{\mathrm{g2}}-\dot{y}_{\mathrm{w2}})+\\
&\quad K_{\mathrm{b}x}b_8(b_8\varphi_{\mathrm{g2}}+b_9\varphi_{\mathrm{w2}})+C_{\mathrm{b}x}b_8(b_8\dot{\varphi}_{\mathrm{g2}}+b_9\dot{\varphi}_{\mathrm{w2}})+\\
&\quad K_{\mathrm{b}x}b_8(b_8\varphi_{\mathrm{g2}}-b_{10}\varphi_{\mathrm{w2}})+C_{\mathrm{b}x}b_8(b_8\dot{\varphi}_{\mathrm{g2}}-b_{10}\dot{\varphi}_{\mathrm{w2}})=0
\end{aligned}\right. \tag{4}$$

(5) The bogie frame:

$$\left\{\begin{aligned}
&M_{\mathrm{b}}\ddot{y}_{\mathrm{b}}+K_{\mathrm{dm}}(y_{\mathrm{b}}+a_2\varphi_{\mathrm{b}}-y_{\mathrm{e2}})+K_{\mathrm{dm}}(y_{\mathrm{b}}+a_2\varphi_{\mathrm{b}}-y_{\mathrm{e3}})+\\
&\quad 2K_{1y}(y_{\mathrm{b}}+a\varphi_{\mathrm{b}}-y_{\mathrm{w1}})+2C_{1y}(\dot{y}_{\mathrm{b}}+a\dot{\varphi}_{\mathrm{b}}-\dot{y}_{\mathrm{w1}})+\\
&\quad 2K_{\mathrm{m}y}(y_{\mathrm{b}}+a_2\varphi_{\mathrm{b}}-y_{\mathrm{m1}}+a_4\varphi_{\mathrm{m1}})+2K_{2y}y_{\mathrm{b}}+\\
&\quad 2K_{1y}(y_{\mathrm{b}}-a\varphi_{\mathrm{b}}-y_{\mathrm{w2}})+2C_{1y}(\dot{y}_{\mathrm{b}}-a\dot{\varphi}_{\mathrm{b}}-\dot{y}_{\mathrm{w2}})+\\
&\quad 2K_{\mathrm{m}y}(y_{\mathrm{b}}-a_2\varphi_{\mathrm{b}}-y_{\mathrm{m2}}-a_4\varphi_{\mathrm{m2}})+2C_{2y}\dot{y}_{\mathrm{b}}+\\
&\quad K_{\mathrm{dt}}(y_{\mathrm{b}}+a_1\varphi_{\mathrm{b}}-y_{\mathrm{d1}})+K_{\mathrm{g}y}(y_{\mathrm{b}}+a_3\varphi_{\mathrm{b}}-y_{\mathrm{g1}}+a_5\varphi_{\mathrm{g1}})+\\
&\quad K_{\mathrm{dt}}(y_{\mathrm{b}}-a_1\varphi_{\mathrm{b}}-y_{\mathrm{d3}})+C_{\mathrm{g}y}(\dot{y}_{\mathrm{b}}+a_3\dot{\varphi}_{\mathrm{b}}-\dot{y}_{\mathrm{g1}}+a_5\dot{\varphi}_{\mathrm{g1}})+\\
&\quad K_{\mathrm{dm}}(y_{\mathrm{b}}-a_2\varphi_{\mathrm{b}}-y_{\mathrm{e6}})+K_{\mathrm{g}y}(y_{\mathrm{b}}-a_3\varphi_{\mathrm{b}}-y_{\mathrm{g2}}-a_5\varphi_{\mathrm{g2}})+\\
&\quad K_{\mathrm{dm}}(y_{\mathrm{b}}-a_2\varphi_{\mathrm{b}}-y_{\mathrm{e7}})+C_{\mathrm{g}y}(\dot{y}_{\mathrm{b}}-a_3\dot{\varphi}_{\mathrm{b}}-\dot{y}_{\mathrm{g2}}-a_5\dot{\varphi}_{\mathrm{g2}})=0\\
&I_{\mathrm{b}}\ddot{\varphi}_{\mathrm{b}}+2K_{\mathrm{g}x}b_4^2\varphi_{\mathrm{b}}+2C_{\mathrm{g}x}b_4^2\dot{\varphi}_{\mathrm{b}}+\\
&\quad 2K_{1x}b_1^2(\varphi_{\mathrm{b}}-\varphi_{\mathrm{w1}})+2C_{1x}b_1^2(\dot{\varphi}_{\mathrm{b}}-\dot{\varphi}_{\mathrm{w1}})+2K_{2x}b_2^2\varphi_{\mathrm{b}}+\\
&\quad 2K_{1x}b_1^2(\varphi_{\mathrm{b}}-\varphi_{\mathrm{w2}})+2C_{1x}b_1^2(\dot{\varphi}_{\mathrm{b}}-\dot{\varphi}_{\mathrm{w2}})+2C_{2x}b_2^2\dot{\varphi}_{\mathrm{b}}+\\
&\quad 2K_{1y}a(y_{\mathrm{b}}+a\varphi_{\mathrm{b}}-y_{\mathrm{w1}})+2C_{1y}a(\dot{y}_{\mathrm{b}}+a\dot{\varphi}_{\mathrm{b}}-\dot{y}_{\mathrm{w1}})-\\
&\quad 2K_{1y}a(y_{\mathrm{b}}-a\varphi_{\mathrm{b}}-y_{\mathrm{w2}})-2C_{1y}a(\dot{y}_{\mathrm{b}}-a\dot{\varphi}_{\mathrm{b}}-\dot{y}_{\mathrm{w2}})+\\
&\quad K_{\mathrm{dt}}a_1(y_{\mathrm{b}}+a_1\varphi_{\mathrm{b}}-y_{\mathrm{d1}})-K_{\mathrm{dt}}a_1(y_{\mathrm{b}}-a_1\varphi_{\mathrm{b}}-y_{\mathrm{d3}})+\\
&\quad 2K_{\mathrm{m}y}a_2(y_{\mathrm{b}}+a_2\varphi_{\mathrm{b}}-y_{\mathrm{m1}}+a_4\varphi_{\mathrm{m1}})+K_{\mathrm{ds}}b_3(b_3\varphi_{\mathrm{b}}-x_{\mathrm{s4}})-\\
&\quad 2K_{\mathrm{m}y}a_2(y_{\mathrm{b}}-a_2\varphi_{\mathrm{b}}-y_{\mathrm{m2}}-a_4\varphi_{\mathrm{m2}})+K_{\mathrm{ds}}b_3(b_3\varphi_{\mathrm{b}}-x_{\mathrm{s2}})+\\
&\quad K_{\mathrm{dm}}a_2(y_{\mathrm{b}}+a_2\varphi_{\mathrm{b}}-y_{\mathrm{e2}})+K_{\mathrm{dm}}a_2(y_{\mathrm{b}}+a_2\varphi_{\mathrm{b}}-y_{\mathrm{e3}})-\\
&\quad K_{\mathrm{dm}}a_2(y_{\mathrm{b}}-a_2\varphi_{\mathrm{b}}-y_{\mathrm{e6}})-K_{\mathrm{dm}}a_2(y_{\mathrm{b}}-a_2\varphi_{\mathrm{b}}-y_{\mathrm{e7}})+\\
&\quad K_{\mathrm{g}y}a_3(y_{\mathrm{b}}+a_3\varphi_{\mathrm{b}}-y_{\mathrm{g1}}+a_5\varphi_{\mathrm{g1}})+K_{\mathrm{m}x}b_5(b_5\varphi_{\mathrm{b}}-b_7\varphi_{\mathrm{m1}})+\\
&\quad C_{\mathrm{g}y}a_3(\dot{y}_{\mathrm{b}}+a_3\dot{\varphi}_{\mathrm{b}}-\dot{y}_{\mathrm{g1}}+a_5\dot{\varphi}_{\mathrm{g1}})+K_{\mathrm{m}x}b_6(b_6\varphi_{\mathrm{b}}-b_7\varphi_{\mathrm{m1}})-\\
&\quad K_{\mathrm{g}y}a_3(y_{\mathrm{b}}-a_3\varphi_{\mathrm{b}}-y_{\mathrm{g2}}-a_5\varphi_{\mathrm{g2}})+C_{\mathrm{m}x}b_6(b_6\dot{\varphi}_{\mathrm{b}}-b_7\dot{\varphi}_{\mathrm{m1}})-\\
&\quad C_{\mathrm{g}y}a_3(\dot{y}_{\mathrm{b}}-a_3\dot{\varphi}_{\mathrm{b}}-\dot{y}_{\mathrm{g2}}-a_5\dot{\varphi}_{\mathrm{g2}})+C_{\mathrm{m}x}b_5(b_5\dot{\varphi}_{\mathrm{b}}-b_7\dot{\varphi}_{\mathrm{m1}})+\\
&\quad K_{\mathrm{m}x}b_5(b_5\varphi_{\mathrm{b}}-b_7\varphi_{\mathrm{m2}})+K_{\mathrm{m}x}b_6(b_6\varphi_{\mathrm{b}}-b_7\varphi_{\mathrm{m2}})+\\
&\quad C_{\mathrm{m}x}b_5(b_5\dot{\varphi}_{\mathrm{b}}-b_7\dot{\varphi}_{\mathrm{m2}})+C_{\mathrm{m}x}b_6(b_6\dot{\varphi}_{\mathrm{b}}-b_7\dot{\varphi}_{\mathrm{m2}})=0
\end{aligned}\right. \tag{5}$$

(6) The first wheel-set:

$$\left\{\begin{aligned}
&M_{\mathrm{w}}\ddot{y}_{\mathrm{w1}}+\frac{W\lambda}{b}y_{\mathrm{w1}}+2f_{22}\left(\frac{\dot{y}_{\mathrm{w1}}}{v}-\varphi_{\mathrm{w1}}\right)-\\
&\quad 2K_{1y}(y_{\mathrm{b}}+a\varphi_{\mathrm{b}}-y_{\mathrm{w1}})-2C_{1y}(\dot{y}_{\mathrm{b}}+a\dot{\varphi}_{\mathrm{b}}-\dot{y}_{\mathrm{w1}})-\\
&\quad 2K_{\mathrm{b}y}(y_{\mathrm{g1}}+a_6\varphi_{\mathrm{g1}}-y_{\mathrm{w1}})-2C_{\mathrm{b}y}(\dot{y}_{\mathrm{g1}}+a_6\dot{\varphi}_{\mathrm{g1}}-\dot{y}_{\mathrm{w1}})=0\\
&I_{\mathrm{w}}\ddot{\varphi}_{\mathrm{w1}}+2f_{11}\left(\frac{b\lambda}{r}y_{\mathrm{w1}}+\frac{b^2\dot{\varphi}_{\mathrm{w1}}}{v}\right)-Wb\lambda\varphi_{\mathrm{w1}}-\\
&\quad 2K_{1x}b_1^2(\varphi_{\mathrm{b}}-\varphi_{\mathrm{w1}})-2C_{1x}b_1^2(\dot{\varphi}_{\mathrm{b}}-\dot{\varphi}_{\mathrm{w1}})-\\
&\quad K_{\mathrm{b}x}b_8(b_8\varphi_{\mathrm{g1}}+b_9\varphi_{\mathrm{w1}})-C_{\mathrm{b}x}b_8(b_8\dot{\varphi}_{\mathrm{g1}}+b_9\dot{\varphi}_{\mathrm{w1}})-\\
&\quad K_{\mathrm{b}x}b_8(b_8\varphi_{\mathrm{g1}}-b_{10}\varphi_{\mathrm{w1}})-C_{\mathrm{b}x}b_8(b_8\dot{\varphi}_{\mathrm{g1}}-b_{10}\dot{\varphi}_{\mathrm{w1}})=0
\end{aligned}\right. \tag{6}$$

(7) The second wheel-set:

$$\left\{\begin{aligned}
&M_{\mathrm{w}}\ddot{y}_{\mathrm{w2}}+\frac{W\lambda}{b}y_{\mathrm{w2}}+2f_{22}\left(\frac{\dot{y}_{\mathrm{w2}}}{v}-\varphi_{\mathrm{w2}}\right)-\\
&\quad 2K_{1y}(y_{\mathrm{b}}-a\varphi_{\mathrm{b}}-y_{\mathrm{w2}})-2C_{1y}(\dot{y}_{\mathrm{b}}-a\dot{\varphi}_{\mathrm{b}}-\dot{y}_{\mathrm{w2}})-\\
&\quad 2K_{\mathrm{b}y}(y_{\mathrm{g2}}-a_6\varphi_{\mathrm{g2}}-y_{\mathrm{w2}})-2C_{\mathrm{b}y}(\dot{y}_{\mathrm{g2}}-a_6\dot{\varphi}_{\mathrm{g2}}-\dot{y}_{\mathrm{w2}})=0\\
&I_{\mathrm{w}}\ddot{\varphi}_{\mathrm{w2}}+2f_{11}\left(\frac{b\lambda}{r}y_{\mathrm{w2}}+\frac{b^2\dot{\varphi}_{\mathrm{w2}}}{v}\right)-Wb\lambda\varphi_{\mathrm{w2}}-\\
&\quad 2K_{1x}b_1^2(\varphi_{\mathrm{b}}-\varphi_{\mathrm{w2}})-2C_{1x}b_1^2(\dot{\varphi}_{\mathrm{b}}-\dot{\varphi}_{\mathrm{w2}})-\\
&\quad K_{\mathrm{b}x}b_8(b_8\varphi_{\mathrm{g2}}+b_9\varphi_{\mathrm{w2}})-C_{\mathrm{b}x}b_8(b_8\dot{\varphi}_{\mathrm{g2}}+b_9\dot{\varphi}_{\mathrm{w2}})-\\
&\quad K_{\mathrm{b}x}b_8(b_8\varphi_{\mathrm{g2}}-b_{10}\varphi_{\mathrm{w2}})-C_{\mathrm{b}x}b_8(b_8\dot{\varphi}_{\mathrm{g2}}-b_{10}\dot{\varphi}_{\mathrm{w2}})=0
\end{aligned}\right. \tag{7}$$

(8) The secondary lateral damper:

$$\left\{\begin{aligned}
&K_{\mathrm{dt}}y_{\mathrm{d2}}+C_{\mathrm{t}}(\dot{y}_{\mathrm{d2}}-\dot{y}_{\mathrm{d1}})=0\\
&C_{\mathrm{t}}(\dot{y}_{\mathrm{d1}}-\dot{y}_{\mathrm{d2}})+K_{\mathrm{dt}}(y_{\mathrm{d1}}-y_{\mathrm{b}}-a_1\varphi_{\mathrm{b}})=0\\
&K_{\mathrm{dt}}y_{\mathrm{d4}}+C_{\mathrm{t}}(\dot{y}_{\mathrm{d4}}-\dot{y}_{\mathrm{d3}})=0\\
&C_{\mathrm{t}}(\dot{y}_{\mathrm{d3}}-\dot{y}_{\mathrm{d4}})+K_{\mathrm{dt}}(y_{\mathrm{d3}}-y_{\mathrm{b}}+a_1\varphi_{\mathrm{b}})=0
\end{aligned}\right. \tag{8}$$

(9) The yaw damper:

$$\left\{\begin{aligned}
&K_{\mathrm{ds}}x_{\mathrm{s1}}+C_{\mathrm{s}}(\dot{x}_{\mathrm{s1}}-\dot{x}_{\mathrm{s2}})=0\\
&C_{\mathrm{s}}(\dot{x}_{\mathrm{s2}}-\dot{x}_{\mathrm{s1}})+K_{\mathrm{ds}}(x_{\mathrm{s2}}-b_3\varphi_{\mathrm{b}})=0\\
&K_{\mathrm{ds}}x_{\mathrm{s3}}+C_{\mathrm{s}}(\dot{x}_{\mathrm{s3}}-\dot{x}_{\mathrm{s4}})=0\\
&C_{\mathrm{s}}(\dot{x}_{\mathrm{s4}}-\dot{x}_{\mathrm{s3}})+K_{\mathrm{ds}}(x_{\mathrm{s4}}-b_3\varphi_{\mathrm{b}})=0
\end{aligned}\right. \tag{9}$$

(10) The first traction motor lateral damper:

$$\left\{\begin{aligned}
&K_{\mathrm{dm}}(y_{\mathrm{e1}}-y_{\mathrm{m1}}+a_4\varphi_{\mathrm{m1}})+C_{\mathrm{my}}(\dot{y}_{\mathrm{e1}}-\dot{y}_{\mathrm{e2}})=0\\
&C_{\mathrm{my}}(\dot{y}_{\mathrm{e2}}-\dot{y}_{\mathrm{e1}})+K_{\mathrm{dm}}(y_{\mathrm{e2}}-y_{\mathrm{b}}-a_2\varphi_{\mathrm{b}})=0\\
&K_{\mathrm{dm}}(y_{\mathrm{e4}}-y_{\mathrm{m1}}+a_4\varphi_{\mathrm{m1}})+C_{\mathrm{my}}(\dot{y}_{\mathrm{e4}}-\dot{y}_{\mathrm{e3}})=0\\
&C_{\mathrm{my}}(\dot{y}_{\mathrm{e3}}-\dot{y}_{\mathrm{e4}})+K_{\mathrm{dm}}(y_{\mathrm{e3}}-y_{\mathrm{b}}-a_2\varphi_{\mathrm{b}})=0
\end{aligned}\right. \tag{10}$$

(11) The second traction motor lateral damper:

$$\left\{\begin{aligned}
&K_{\mathrm{dm}}(y_{\mathrm{e5}}-y_{\mathrm{m2}}-a_4\varphi_{\mathrm{m2}})+C_{\mathrm{my}}(\dot{y}_{\mathrm{e5}}-\dot{y}_{\mathrm{e6}})=0\\
&C_{\mathrm{my}}(\dot{y}_{\mathrm{e6}}-\dot{y}_{\mathrm{e5}})+K_{\mathrm{dm}}(y_{\mathrm{e6}}-y_{\mathrm{b}}+a_2\varphi_{\mathrm{b}})=0\\
&K_{\mathrm{dm}}(y_{\mathrm{e8}}-y_{\mathrm{m2}}-a_4\varphi_{\mathrm{m2}})+C_{\mathrm{my}}(\dot{y}_{\mathrm{e8}}-\dot{y}_{\mathrm{e7}})=0\\
&C_{\mathrm{my}}(\dot{y}_{\mathrm{e7}}-\dot{y}_{\mathrm{e8}})+K_{\mathrm{dm}}(y_{\mathrm{e7}}-y_{\mathrm{b}}+a_2\varphi_{\mathrm{b}})=0
\end{aligned}\right. \tag{11}$$

In the above equation, r represents wheel's rolling radius, W denotes axle load, λ represents wheel tread's equivalent taper, f_{11} and f_{22} represent the longitudinal and lateral creep coefficients. Here, f_{11} and f_{22} can be represented as [18]

$$f_{11}=GabC_{11},\ f_{22}=GabC_{22} \tag{12}$$

in which, G denotes wheel-rail material's shear modulus, C_{11} and C_{22} represent Kalker coefficients, a and b represent wheel-rail contact ellipse's long and short half axes.

$$a=m\left[\frac{3\pi Nk}{4A}\right]^{1/3},\quad b=n\left[\frac{3\pi Nk}{4A}\right]^{1/3} \tag{13}$$

Here, $N=(M_{\mathrm{c}}/2+M_{\mathrm{b}}+2M_{\mathrm{w}}+2M_{\mathrm{m}}+2M_{\mathrm{g}})g/4$, M_{c} is the car body mass, $g=9.8$ m/s^2; $A=(1/R_{\mathrm{r1}}+1/R_{\mathrm{r2}}+1/R_{\mathrm{w1}}+1/R_{\mathrm{w2}})/2$, R_{r1}, R_{r2} and R_{w1}, R_{w2} are the principal curvature radii of the rail head ellipsoid and wheel tread ellipsoid; $k=2(1-\mu^2)/(\pi E)$, E denotes wheel-rail material's elastic modulus, μ represents wheel-rail material's Poisson ratio; m and n are constants related to $\beta=\arccos(B/A)$; $B=(1/R_{\mathrm{r1}}-1/R_{\mathrm{r2}}+1/R_{\mathrm{w1}}-1/R_{\mathrm{w2}})/2$.

III. Stability Analysis Method

At present, there are mainly two methods employed to assess railway vehicle's hunting stability, i.e., the linear and nonlinear critical velocity (CV) methods [12]. Although there are certain differences in the stability results of vehicles analyzed by these two methods, considering the prominent advantages of linear CV analysis method, such as high computational efficiency and ease of analyzing the impact of parameter changes, it is very suitable for early regularity exploration work [16,19]. Therefore, it has been extensively used in bogie's hunting motion stability analysis. In view of this, based on the Routh-Hurwitz stability criterion [5,13], by analyzing the linear CV characteristics of the PB systems, the dynamic relationship between the traction transmission components and PB system's hunting stability is explored. Here, the specific solving process for linear CV is as follows:

Perform Laplace transform on equations (1) to (11) (i.e., substitute $\ddot{y}_i = s^2 y_i$, $\dot{y}_i = s y_i$, $\ddot{\varphi}_i = s^2\varphi_i$, $\dot{\varphi}_i = s\varphi_i$, and $\dot{y}_j = s y_j$ into equations (1) to (11) respectively, where subscripts i= m1, m2, b, g1, g2, w1, w2; j=e1~e8, s1~s4, d1~d4, s represents complex variables), and express them in the following matrix form

$$\boldsymbol{AX} = 0 \tag{14}$$

In the formula, $\boldsymbol{A}$ is the coefficient matrix of the $\boldsymbol{X}$ vector containing the complex variable s; $\boldsymbol{X}$=[y_{m1} φ_{m1} y_{m2} φ_{m2} y_b φ_b y_{g1} φ_{g1} y_{g2} φ_{g2} y_{w1} φ_{w1} y_{w2} φ_{w2} y_{e1} y_{e2} y_{e3} y_{e4} y_{e5} y_{e6} y_{e7} y_{e8} x_{s1} x_{s2} x_{s3} x_{s4} y_{d1} y_{d2} y_{d3} y_{d4}]$^{\mathrm{T}}$.

According to equation (14), make the determinant of the coefficient matrix $\boldsymbol{A}$ equal to 0, that is, $|A|_{30\times30}= 0$, and expand the complex variable s from high to low order to obtain its Hurwitz stability criterion characteristic equation, as follows

$$\sum_{k=0}^{36} e_k s^{36-k} = 0 \tag{15}$$

in which, e_k is the coefficient of the complex variable s of each order, k=0,1,2⋯,36.

Let the determinant value of each coefficient e_k in equation (15) be equal to 0, the following equation will be obtained

$$\begin{vmatrix} e_1 & e_3 & \cdots & e_{2n-1} & 0 & \cdots & 0 \\ e_0 & e_2 & \cdots & e_{2n} & 0 & \cdots & 0 \\ 0 & e_1 & e_3 & \cdots & e_{2n-1} & \cdots & 0 \\ \cdots & \cdots & \cdots & \cdots & \cdots & \cdots & \cdots \\ 0 & \cdots & 0 & e_0 & e_2 & \cdots & e_{2n} \end{vmatrix}_{36\times36} = 0, n = \begin{cases} 1\sim18, \text{Odd subscript} \\ 0\sim18, \text{Even subscript} \end{cases} \tag{16}$$

By transforming the real and imaginary parts of the root Δ in equation (16), the vibration frequency f and damping ratio ξ of each mode can be obtained, where f=Im(Δ)/(2π), ξ=Re(Δ)/|Δ|, Im and Re represent taking the real and imaginary parts. At a certain speed, when ξ>0, it indicates that the PB system is unstable, ξ<0 indicates that the PB is stable, and the train speed at ξ=0 is the PB system's hunting motion CV i.e., v_c.

IV. Validation of the Hunting Motion Model

For the purpose of verifying the established PB hunting motion model's correctness, a high-speed train's dynamics model is established by using the dynamics software SIMPACK, as illustrated in Figure 2 (in which this model's correctness has already been verified using the measured data provided in reference [20]), and the analysis results obtained from SIMPACK simulation are compared with those of this paper's model. The main parameter values of the PB system can be seen in Table I.

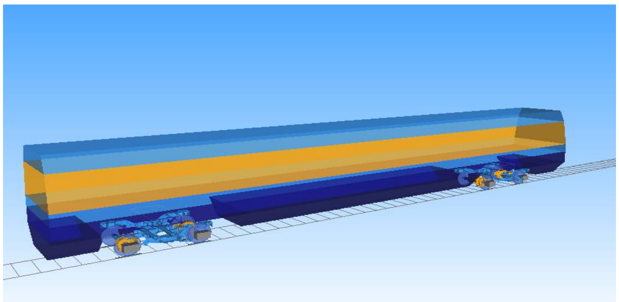

Fig. 2. SIMPACK vehicle dynamics model

TABLE I
SYSTEM PARAMETER VALUES

Parameter	Unit	Value
M_b	kg	3 200
M_w	kg	1 870
M_m	kg	800
M_g	kg	288
I_b	kg·m^2	3 200
I_w	kg·m^2	587
I_m	kg·m^2	85
I_g	kg·m^2	23.7
K_{1x}	N/m	1.47×10^7
K_{1y}	N/m	6.5×10^6
K_{2x}	N/m	1.735×10^5
K_{2y}	N/m	1.735×10^5
C_{1x}	N·s/m	5 000
C_{1y}	N·s/m	5 000
C_{2x}	N·s/m	6 000
C_{2y}	N·s/m	6 000
C_s	N·s/m	25 300
C_t	N·s/m	20 000
C_{my}	N·s/m	4 000
K_{gx}	N/m	5×10^6
K_{gy}	N/m	5×10^6
C_{gx}	N·s/m	1 000
C_{gy}	N·s/m	1 000
K_{mx}	N/m	7.35×10^6
K_{my}	N/m	100 000
C_{mx}	N·s/m	1 000
K_{bx}	N/m	1.15×10^7
K_{by}	N/m	1.15×10^7
C_{bx}	N·s/m	100
C_{by}	N·s/m	100
K_p	N/m	1.0×10^6
$K_{p\varphi}$	N.m/rad	1.0×10^6
C_p	N·s/m	100
$C_{p\varphi}$	N·s.m/rad	100

Table II presents the comparison results of the PB hunting motion's CV under different traction motor suspension lateral stiffness obtained from SIMPACK simulation model and this paper model. As displayed in Table II, the CV values of the PB system's hunting motion under the two models have good consistency, with a relative deviation of less than 7%. The results show that, the PB hunting motion model considering traction transmission components' coupling effect established in this paper is correct, providing a model reference for PB system's hunting motion stability analysis.

TABLE II
COMPARISON BETWEEN CALCULATION RESULTS AND VEHICLE SIMULATION RESULTS

K_{my}/(N/m)	v_c/(km/h)		Deviation/%
	Model in this paper	Vehicle simulation	
10 000	397.54	415.26	4.27
25 000	401.14	418.37	4.12
50 000	407.40	423.51	3.80
100 000	420.96	438.90	4.09
200 000	452.10	481.13	6.03
300 000	307.78	325.66	5.49
400 000	291.26	307.50	5.28
500 000	286.58	301.75	5.03

V. THE EFFECT OF TRACTION TRANSMISSION SYSTEM'S ISOLATION PARAMETERS ON PB SYSTEM'S HUNTING STABILITY

The key to designing the isolation system for traction motors and gearboxes is to investigate the dynamic relationship between the traction transmission system's isolation parameters and the PB system's hunting motion stability. This section uses the established PB hunting motion model considering the influence of traction transmission components, taking the PB system shown in Table I as the research object, to study the influences of the traction motor and gearbox's suspension parameters and coupling's performance parameters on the PB system's hunting motion stability.

A. The dynamic effect between traction motor suspension parameters and PB system's hunting motion

Figure 3 displays the variation law of PB hunting motion's CV under different traction motor suspension stiffness.

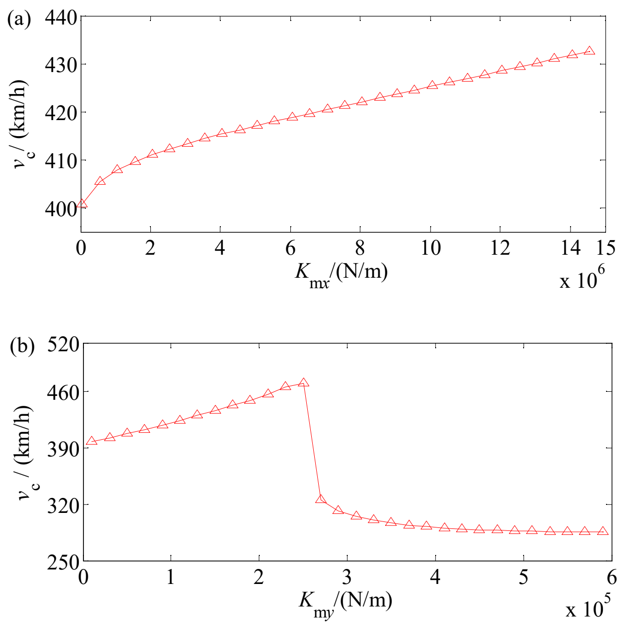

Fig. 3. The variation law of PB hunting motion's CV under different traction motor suspension stiffness: (a) the influence of longitudinal stiffness K_{mx}; (b) the influence of lateral stiffness K_{my}

As displayed in Figure 3, as traction motor suspension's longitudinal stiffness increases, the PB system's hunting motion CV gradually increases, that is, a larger traction motor suspension longitudinal stiffness is beneficial to improve PB system's hunting stability. Additionally, as traction motor suspension's lateral stiffness increases, the PB system's hunting motion CV first increases, then decreases, and finally stabilizes. In other words, there exists an optimal traction motor suspension lateral stiffness, which can ensure that the PB system has the best stability at this stiffness value. Compared with large stiffness values, when the lateral stiffness is less than the optimal value, the PB system can have a better stability performance. Therefore, when designing traction motor suspension's lateral stiffness, it should be avoided to design it too large.

Figure 4 shows the variation law of PB hunting motion's CV under different traction motor suspension damping.

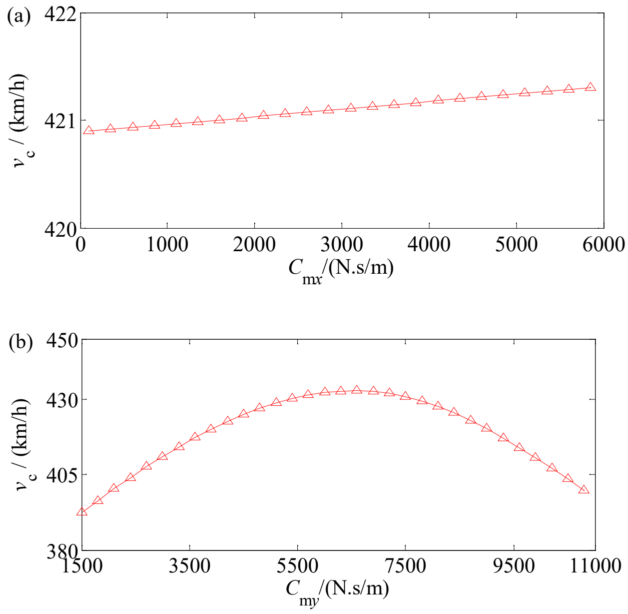

Fig. 4. The variation law of PB hunting motion's CV under different traction motor suspension damping: (a) the influence of longitudinal damping C_{mx}; (b) the influence of lateral damping C_{my}

As shown in Figure 4, with the increase of the traction motor suspension's longitudinal damping, the PB system's hunting motion CV slightly increases, and the overall change is not significant, with a relatively weak impact. Similar to the influence law of its lateral stiffness, as traction motor suspension's lateral damping increases, the PB system's hunting motion CV first increases and then decreases, and the system's stability first improves and then deteriorates. That is, there exists an optimal traction motor suspension lateral damping value, which can ensure that the PB system has the best stability at this damping value.

By comprehensively analyzing Figures 3 and 4, we can see clearly that, for the purpose of achieving a good stability performance for PB system's hunting motion, a larger longitudinal stiffness should be reasonably selected when designing traction motor's suspension systems. In addition, we should pay particular attention to matching the traction motor suspension system with an appropriate lateral stiffness and lateral damping.

B. The dynamic effect between gearbox suspension parameters and PB system's hunting motion

Figure 5 displays the variation law of PB hunting motion's CV under different gearbox suspension stiffness.

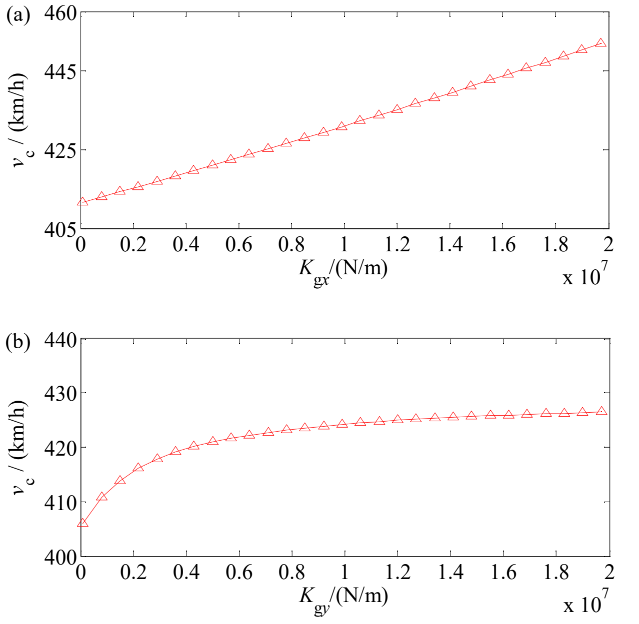

Fig. 5. The variation law of PB hunting motion's CV under different gearbox suspension stiffness: (a) the influence of longitudinal stiffness K_{gx}; (b) the influence of lateral stiffness K_{gy}

From Figure 5, we can see clearly that, as gearbox suspension's longitudinal stiffness increases, the PB system's hunting motion CV gradually increases. In other words, a larger gearbox suspension longitudinal stiffness is beneficial to improve PB system's hunting stability. Furthermore, as gearbox suspension's lateral stiffness increases, the PB system's hunting motion CV gradually increases and then tends to stabilize. Overall, when gearbox suspension's lateral stiffness value increases to a certain extent, the PB system's stability no longer undergoes significant changes.

Figure 6 shows the variation law of PB hunting motion's CV under different gearbox suspension damping. As displayed in the figure, as gearbox suspension's longitudinal damping increases, the PB system's hunting motion CV slightly increases, and the PB system's stability performance is improved. The gearbox suspension's lateral damping has almost no effect on PB system's hunting stability. Combined with Figure 5, it is not difficult to find that, gearbox suspension's stiffness has a greater impact on PB system's stability than damping. In other words, when designing the gearbox suspension system, we need to pay special attention to the design of its stiffness parameters.

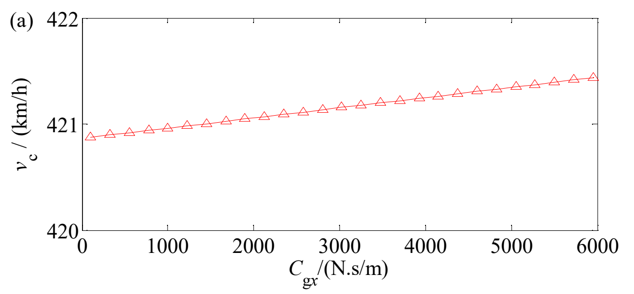

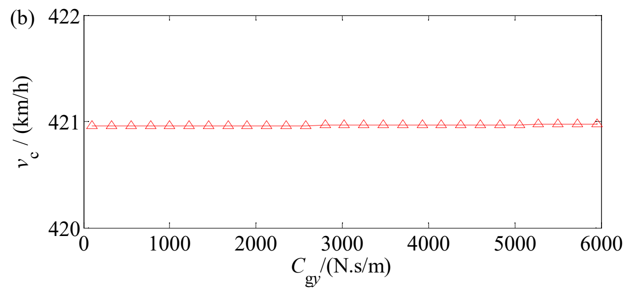

Fig. 6. The variation law of PB hunting motion's CV under different gearbox suspension damping: (a) the influence of longitudinal damping C_{gx}; (b) the influence of lateral damping C_{gy}

C. The dynamic effect between coupling performance parameters and PB system's hunting motion

Figure 7 shows the variation law of PB hunting motion's CV under different coupling stiffness.

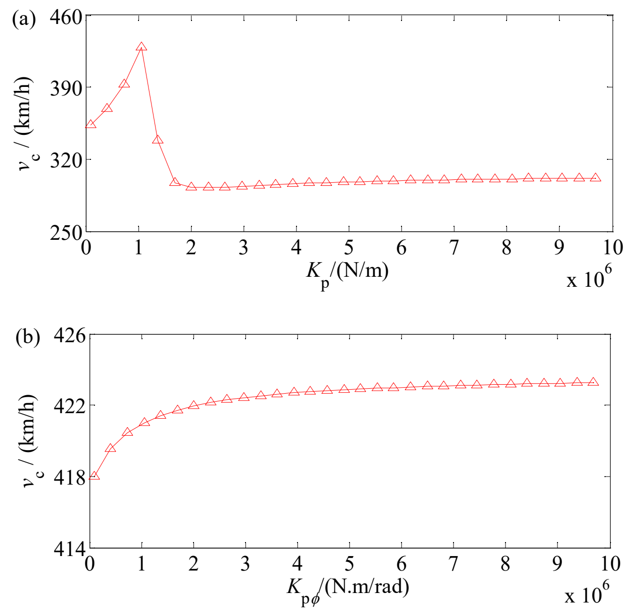

Fig. 7. The variation law of PB hunting motion's CV under different coupling stiffness: (a) the influence of lateral stiffness K_p; (b) the influence of yaw stiffness $K_{p\varphi}$

According to Figure 7 (a), we can see clearly that, the influence of coupling's lateral stiffness on PB system's stability is basically consistent with the traction motor suspension lateral stiffness. That is, as the lateral stiffness of the coupling increases, the PB system's hunting motion CV first increases and then decreases, and finally tends to stabilize. There is an optimal coupling lateral stiffness, which makes the system most stable at this stiffness value. In addition, on the side smaller than the optimal stiffness value, the PB system has a higher CV and better system stability. When the lateral stiffness of the coupling is greater than this optimal value, the PB system's hunting motion CV significantly decreases, namely, the system's stability deteriorates. The reason for this situation is that, when the coupling's lateral stiffness is greater than a certain value, the traction motor and gearbox are equivalent to being rigidly connected together. In this case, if the suspension stiffness value between the gearbox itself and the frame is large, the equivalent mass shared by the traction motor and gearbox as a whole on the frame will increase, thereby leading to a deterioration in PB system's stability. In addition, by analyzing Figure 7 (b), we can see clearly that, as the coupling's yaw stiffness increases, the PB system's hunting motion CV first gradually increases and then tends to stabilize, but the overall change is not significant. Therefore, a larger coupling yaw stiffness is beneficial to improve PB system's hunting stability.

Figure 8 displays the variation law of PB hunting motion's CV under different coupling damping.

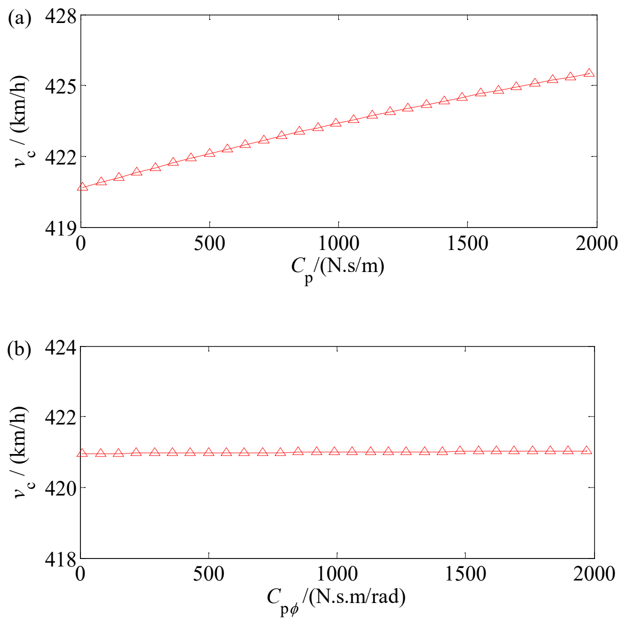

Fig. 8. The variation law of PB hunting motion's CV under different coupling damping: (a) the influence of lateral damping C_p; (b) the influence of yaw damping $C_{p\varphi}$

As shown in Figure 8, as coupling's lateral damping increases, the PB system's hunting motion CV increases and the system's stability improves. Moreover, as coupling's yaw damping increases, the PB system's hunting motion CV remains almost unchanged. In other words, the coupling yaw damping has little impact on PB system's stability. From the comprehensive analysis of Figures 7 and 8, it can be seen that, among the numerous performance parameters of the coupling, its lateral stiffness has the greatest impact on PB system's stability, followed by the yaw stiffness, lateral damping, the yaw damping having the smallest impact. In order to ensure that the PB has a good stability, on the premise of matching a larger yaw stiffness value, we particularly need to pay attention to the design of the coupling's lateral stiffness.

It can be seen from the above analysis that, each traction transmission component and its vibration isolation parameters have a certain influence on PB system's hunting stability. For the purpose of obtaining a more accurate stability analysis results for high-speed train's PB system, and providing a model reference for PB system's hunting stability analysis as well as a theoretical guidance for the design of traction motor and gearbox's suspension parameters, it is necessary to integrate each traction transmission component with the bogie frame into a whole system for research.

VI. Conclusions

In this paper, a high-speed train's PB hunting motion model that comprehensively considers the coupling interaction between the traction motor, gearbox, and bogie frame is proposed. The model is verified through vehicle simulation. Based on this, the influences of traction motor and gearbox's vibration isolation parameters as well as the coupling's performance parameters on PB system's hunting stability are explored. The main conclusions are as follows:

1) The traction motor suspension parameters have a significant impact on PB system's hunting motion stability. To achieve a good stability, when designing the traction motor's suspension system, a larger longitudinal stiffness should be reasonably selected. In addition, special attention should be paid to matching an appropriate lateral stiffness and lateral damping.
2) The gearbox suspension parameters have a certain impact on PB system's hunting motion stability, and its stiffness parameters have a more significant effect than damping. When designing gearbox's suspension system, special attention should be paid to the design of its stiffness parameters, meanwhile, the stiffness design value should meet a certain order of magnitude and cannot be selected too small.
3) The coupling's performance parameters have a certain impact on PB system's hunting motion stability. Among the numerous performance parameters of the coupling, its lateral stiffness has the greatest impact on system stability, followed by the yaw stiffness, lateral damping, the yaw damping having the smallest impact. In order to ensure that the PB has a good stability, on the premise of matching a larger yaw stiffness value, special attention should be paid to the design of its lateral stiffness.

This study provides a model reference for PB system's hunting motion stability analysis, and also provides a theoretical guidance for the design of traction motor and gearbox's suspension parameters.

References

[1] H. Zhang, L. Ling and W. M. Zhai, "Adaptive nonlinear damping control of active secondary suspension for hunting stability of high–speed trains," *Applied Mathematical Modelling*, vol. 133, pp. 79–107, 2024.

[2] F. Gan, H. Y. Dai, G. B. Luo, Z. H. Yang and T. Li, "Spectrum analysis of hunting motion of flexible bogies in high–speed EMUs," *Journal of Traffic and Transportation Engineering*, vol. 22, no. 1, pp. 155–167, 2022.

[3] Y. Yan and J. Zeng, "Hopf bifurcation analysis of railway bogie," *Nonlinear Dynamics*, vol. 92, no. 1, pp. 1–11, 2017.

[4] H. M. Sedighi and K. H. Shirazi, "Bifurcation analysis in hunting dynamical behavior in a railway bogie:Using novel exact equivalent functions for discontinuous nonlinearities," *Scientia Iranica*, vol. 19, no. 6, pp. 1493–1501, 2012.

[5] Y. W. Yu, C. C. Zhou and L. L. Zhao, "Analytical research of yaw damper damping matching for high-speed train," *Journal of Mechanical Engineering*, vol. 54, no. 2, pp. 159–168, 2018.

[6] Y. Q. Shi, J. H. Yang and G. W. Luo, "Hunting patterns and bifurcation characteristics of a railway bogie on curved track," *Journal of the China Railway Society*, vol. 46, no. 8, pp. 37–47, 2024.

[7] K. Xu, J. Zeng and C. H. Huang, "Nonlinear stability analysis of motor bogies for high–speed trains," *Proceedings of the Institution of Mechanical Engineers, Part F: Journal of Rail and Rapid Transit*, vol. 233, no. 9, pp. 885–895, 2018.

[8] C. H. Huang, C. Y. Song, J. Fan and J. Zeng, "Analysis on hunting frequency jump phenomenon of high–speed bogies with elastic motor suspension," *Journal of the China Railway Society*, vol. 43, no. 10, pp. 20–28, 2021.

[9] Z. W. Feng, H. D. Hu, Z. H. Yang C. H. Huang, B. Zheng and J. Zeng, "Bogie stability and control strategy based on motor suspension," *Journal of Traffic and Transportation Engineering*, vol. 24, no. 2, pp. 152–165, 2024.

[10] Y. YAO, G. S. Wu, Y. Sardahi and J. Q. Sun, "Hunting stability analysis of high–speed train bogie under the frame lateral vibration active control," *Vehicle System Dynamics*, vol. 56, no. 2, pp. 297–318, 2017.

[11] X. X. Zhang, G. S. Wu, G. Li and Y. Yao, "Actuator optimal placement studies of high–speed power bogie for active hunting stability," *Vehicle System Dynamics*, vol. 58, no. 1, pp. 108–122, 2019.

[12] K. Xu, J. Zeng, C. H. Huang and Y. Y. Qi, "Influenceof suspension parameters of traction motor on stability of high speed train bogie," *Journal of the China Railway Society*, vol. 41, no. 8, pp. 32–38, 2019.

[13] Y. W. Yu, J. Y. Wang, Y. P. Song and L. L. Zhao, "Stability analysis of power bogie system and forward design of its yaw damper damping parameter," *Engineering Letters*, vol. 31, no. 4, pp. 1434–1441, 2023.

[14] Z. W. Wang, G. M. Mei, Q. Xiong Q, Z. H. Yin and W. H. Zhang, "Motor car–track spatial coupled dynamics model of a high–speed train with traction transmission systems," *Mechanism and Machine Theory*, vol. 137, pp. 386–403, 2019.

[15] G. Sun, Z. S. Ren, X. Xin and X. Wei, "Dynamics of gear transmission system of high–speed vehicle," *Journal of Mechanical Engineering*, vol. 55, no. 18, pp. 104–111, 2019.

[16] W. B. Huo, C. H. Huang, H. D. Hu, Z. H. Yang and B. Zheng, "Study on dynamic performance of EMU bogies with motor active suspensions," *Journal of the China Railway Society*, vol. 47, no. 2, pp. 43–54, 2025.

[17] Y. W. Yu, Y. P. Song, L. L. Zhao and C. C. Zhou, "Numerical investigation on train vertical dynamics with damper rubber joint stiffness," *IAENG International Journal of Applied Mathematics*, vol. 53, no. 1, pp. 122–129, 2023.

[18] W. M. Zhai, *Vehicle-track coupled dynamics*, *Fourth edition*. Science Press, Beijing, 2015.

[19] C. H. Huang, S. L. Liang, J. Zeng, J. Fan and C. Y. Song, "Effect of the suspension parameter of traction motors on the stability of motor car bogies," *Rolling Stock*, vol. 52, no. 11, pp. 1–5, 2014.

[20] W. M. Zhai, P. F. Liu, J. H. Lin and K. Y. Wang, "Experimental investigation on vibration behaviour of a CRH train at speed of 350 km/h," *International Journal of Rail Transportation*, vol. 3, no. 1, pp. 1–16, 2015.